analytical chemistry

pubs.acs.org/ac Article

Advancing Orbitrap Measurements of Collision Cross Sections to Multiple Species for Broad Applications

Virginia K. James, James D. Sanders, Konstantin Aizikov, Kyle L. Fort, Dmitry Grinfeld, Alexander Makarov, and Jennifer S. Brodbelt*

Cite This: *Anal. Chem.* 2022, 94, 15613−15620 Read Online

ACCESS | Metrics & More | Article Recommendations | Supporting Information

ABSTRACT: Measurement of collision cross section (CCS), a parameter reflecting an ion's size and shape, alongside high-resolution mass analysis extends the depth of molecular analysis by providing structural information beyond molecular mass alone. Although these measurements are most commonly undertaken using a dedicated ion mobility cell coupled to a mass spectrometer, alternative methods have emerged to extract CCSs directly by analysis of the decay rates of either time-domain transient signals or the FWHM of frequency domain peaks in FT mass analyzers. This information is also accessible from FTMS mass spectra obtained in commonly used workflows directly without the explicit access to transient or complex Fourier spectra. Previously, these experiments required isolation of individual charge states of ions prior to CCS analysis, limiting throughput. Here we advance Orbitrap CCS measurements to more users and applications by determining CCSs from commonly available mass spectra files as well as estimating CCS for multiple charge states simultaneously and showcase these methods by the measurement of CCSs of fragment ions produced from collisional activation of proteins.

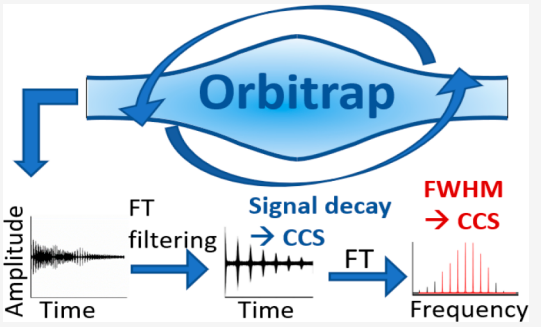

INTRODUCTION

In the effort to develop more accurate and higher-resolution methods to characterize molecules in complex mixtures by mass spectrometry, the measurement of additional physiochemical parameters, such as collision cross section, offers an additional degree of structural specificity. The collision cross section (CCS) is a quantitative description of the size and shape of an ion, more explicitly described as the rotational average of the combined radii of two colliding molecules.[1−3] Although CCSs have been determined for countless types and classes of molecules, CCS measurements have shown exceptional utility in the characterization of proteins,[4,5] as many proteins adopt diverse tertiary structures that may be profiled based on variations in the CCSs.[6] Determination of CCSs facilitates prediction of three-dimensional models of proteins and allows development of correlations between gas-phase structures and those in solution. The impact of protein conformations on ligand binding and protein−protein interactions contributes to many critical biological outcomes, such as the progression of disease states, viral membrane fusion, and enzymatic activity.[7−9] This has spurred significant interest in the development of new ways to measure CCSs with greater sensitivity, higher throughput, and for even larger macromolecules.

While CCS measurements are typically performed using ion mobility (IM) spectrometers such as ones based on low field drift tubes,[4,10,11] alternative methods have been employed based on algorithms that estimate CCS from the signal decay rates in ion trapping analyzers either in the time or frequency domain.[12−17] Such approaches are generally based on the correlation between ion-neutral collision rates and cross sections, thus deriving insight from the decay of ion signals with time.[18−21] These types of alternative CCS measurements have been implemented using both high-resolution (ion cyclotron resonance (ICR) systems[13−17] and Orbitrap analyzers[12]) and low-resolution (electrostatic linear ion trap[22]) Fourier transform (FT) mass analyzers as well as a home-built charge detection mass spectrometer.[23] CCS measurements were first reported using FT-ICR mass spectrometers several decades ago,[18−21] and a more recent strategy adapted for FT-ICR instruments developed a relationship between the full width half-maximum (FWHM) of the frequency domain peak ($\Delta\omega$) and CCS (σ) (eq 1) derived from the hard-sphere collision model description of ion-neutral collisions.[13−15,24]

Received: May 17, 2022
Accepted: October 20, 2022
Published: November 3, 2022

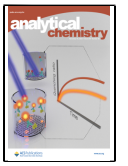

https://doi.org/10.1021/acs.analchem.2c02146
Anal. Chem. 2022, 94, 15613−15620

$$\sigma = \frac{\Delta\omega}{N\nu} \quad (1)$$

To establish this relationship, the ion's speed (ν) and the pressure within the ICR cell must also be defined, the latter of which was used to calculate the density of neutral gas molecules (N).[16] This method has been employed for determination of CCSs of a wide array of analytes ranging from small molecules[14,15,25] to proteins[16] and more recently has been used to study structural changes upon binding of alkali metal ions to the peptide leucine enkephalin and a macrocyclic cryptand as well as measure CCSs of product ions generated from collisional activated dissociation of the complexes.[26] The possibility of measuring CCS by using an Orbitrap mass spectrometer was first proposed in 2009, in which it was surmised that relative CCSs could be determined by the rate of transient signal decay in the time domain (eq 2), where c represents the decay constant and N_o represents the number of ions at time zero.[27] This decay constant along with the ion's path length (l) and frequency (f_0) may be used to calculate CCS as shown in eq 3.

$$N(t) = N_o e^{-ct} \quad (2)$$

$$\sigma = \frac{c}{lf_0 N} \quad (3)$$

A similar concept was implemented experimentally on an FT-ICR platform,[17] demonstrating the measurements of CCSs of ubiquitin that matched closely to values determined by IM. This type of CCS method was also successfully used to monitor the unfolding of protein ions following irradiation by a tunable IR laser in an FT-ICR system.[28] Recently, the time-domain decay rate method was demonstrated experimentally on an Orbitrap mass analyzer, facilitated by development of a computational method termed direct decay profile fitting.[12] In essence, Fourier transformation of the transient data followed by inverse FT allowed the final time-domain data to be fit to an exponential decay model to determine the decay rate.[12] Another key step in this prior study was the implementation of a pressure calibration as the pressure within the Orbitrap chamber is not known with sufficient precision.[12] From IM studies, the 9+ charge state of ubiquitin is known to adopt a single conformation,[4] so this ion's decay rate and IM CCS were used to calibrate the pressure for the determination of Orbitrap CCSs.[12] With appropriate calibration, the direct decay profile fitting method was used to measure CCSs of a series of proteins as large as myoglobin (16.9 kDa) in both high charge states (denatured) and low charge states (native-like).[12] The CCSs determined by this method agreed with CCS values measured by IM with a maximum deviation of 7% for ions that adopt a single conformation.[12] While this error tolerance is not within that of IM systems (1−2%), it must also be considered that collisions between ions and neutrals in IM systems are low energy and numerous, dampening the kinetic energy of ions and entailing long-range interactions, which can depend on properties of drift gas such as polarizability (Langevin model).[29−31] In some cases, these collisions with momentum transfer may cause internal heating of the ion, thus leading to unfolding and overestimated CCSs.[17] Conversely, in FT-MS (both Orbitrap and FT-ICR) systems, energies of collisions are much higher (approximately 4 keV per charge). Owing to this high kinetic energy, we assume that each ion-neutral collision induces fragmentation of an ion (for ions that are less than m/z 2000), thus causing its removal from the original ion packet, resulting in signal decay.[12] As the ions have such high kinetic energies in an Orbitrap, they are not likely to experience long-range interactions as this energy regime eliminates effects from properties such as polarization of the ion and/or drift gas, thus following the hard-sphere collision model.[12,17,32] Therefore, owing to the differing energy regimes of the two measurement systems (ion mobility versus Orbitrap analyzer), exact equality between measured CCSs is not expected, and Orbitrap CCSs may even be underestimated relative to IM CCS values.[12]

Although all previously described methods rely on the transient or complex Fourier spectral information, one can alternatively utilize mass spectra directly for CCS measurement. Circumventing the need for transient files and instead calculating CCS from common MS data file formats (*i.e.*, RAW files)[33] significantly increase accessibility and practicality of the method for large data sets, thus expanding Orbitrap CCS measurements to a wider range of applications and users. Additionally, many of the previously described methods relied on isolating a single charge state of an ion of interest in the mass spectrometer per experiment, therefore limiting throughput. Other new data processing techniques have reported simultaneous measurement of CCS of small molecules in low charge states on FT-ICR platforms.[24,34]

Here we develop and evaluate alternate computational methods with the goal of estimating CCS from commonly available mass spectra files instead of transients on an Orbitrap mass spectrometer. To accomplish this goal, we compare the FWHM and direct decay profile fitting methods as well as a method adapted from the direct decay profile fitting method for data input from raw files (Scheme S1). To increase throughput, we probe an alternative method of data analysis to obtain CCSs of multiple ions of different m/z simultaneously, termed the wide-selected ion monitoring (wide-SIM) direct decay profile fitting method. The wide-SIM method allows the determination of CCS for situations in which isolation of specific ions or charge states is not possible and also reduces the data acquisition time when monitoring CCS of multiple charge states or proteins. Accomplishment of both goals (accessibility to users and higher-throughput multiplex CCS measurement) enables broader adoption of Orbitrap CCS methods by a greater community of users and for a larger range of applications.

METHODS AND MATERIALS

Instrumentation. With a few exceptions, most experiments were performed on a Thermo Scientific Orbitrap Elite mass spectrometer (Bremen, Germany), which was equipped with a custom pressure regulator to control the flow of N_2 collision gas to the HCD cell as previously described.[12] CCS measurements for fragment ions and collision induced unfolding (CIU) of cytochrome c were performed on a Orbitrap Q-Exactive HF-X with Biopharma option. Further details on instrumentation, data acquisition, and processing including a scheme outlining data processing for each method (Scheme S1) and materials are provided in the Supporting Information.

RESULTS AND DISCUSSION

Orbitrap CCSs from Mass Spectra. *FWHM Method.* When approaching the goal of Orbitrap CCS determination

https://doi.org/10.1021/acs.analchem.2c02146
Anal. Chem. 2022, 94, 15613−15620

directly from mass spectra instead of from transients, we first examined an alternative computational method developed in FT-ICR experiments, in which the FWHM of the frequency domain peak is used to derive the decay rate.[13−17,35] In addition to a being a potentially promising method for determining CCS from mass spectra using an Orbitrap analyzer, this FWHM method also provides a more direct comparison to CCSs measured in an FT-ICR system. Since the collisional decay in both Orbitrap and FT-ICR systems is exponential, a Lorentzian peak shape model can be applied to the peak in the absorption mode to determine the FWHM. The FWHM of the seven most abundant peaks can then be averaged. Through the formula for Lorentzian peak shape (eq 4), in which f is the frequency at which the spectral amplitude is observed and f_0 represents the centroid frequency of the peak, the relationship between the rate of transient signal decay and the FWHM[13−15,22] (eq 5) can be determined and thus may be employed to find the CCS. The relationship shown in eq 3 yields a good approximation of CCS provided that the transient is sufficiently long and shows ample signal decay.[36]

$$L(f) = \frac{1}{4\pi^2(f - f_0)^2 + c^2} \tag{4}$$

$$\text{FWHM} = \frac{c}{\pi} \tag{5}$$

This method for obtaining signal decay rates was of interest as the FWHM method offers the potential to provide CCS measurements simultaneously with the collection of mass spectra. In the Orbitrap analyzer, the ion's m/z is related to the frequency (eq 6), and the constant (const) is determined by calibration of the instrument with ions of precisely known m/z. Therefore, the frequency FWHM is proportional to the peak width in the mass spectrum (eq 7).

$$m/z = \text{const}/f_0^2 \tag{6}$$

$$\frac{\text{FWHM}}{f_0} = \frac{1}{2}\frac{\Delta(m/z)}{m/z} \tag{7}$$

The estimated decay constant c is related to the ion's collision cross section (σ) (eq 8) where N is the concentration of gas molecules and l is the average ion path per one oscillation.

$$c = lf_0N\sigma \tag{8}$$

For the Orbitrap analyzers of the high-field family, the average ion path l is around 60 mm (unlike in the FT ICR, the ion's velocity is not constant in the Orbitrap analyzer). Finally, FWHM of the mass spectrum peak can be related to the collision cross section by substitution of the frequency FWHM formula (eq 6) to give eq 9.

$$\sigma = \frac{c}{lf_0N} = \frac{\pi}{2lN}\frac{\Delta(m/z)}{m/z} \tag{9}$$

We compared the FWHM and direct decay profile fitting methods to evaluate their applications. When first applying the FWHM method to Orbitrap data, we attempted to process FT data in magnitude mode, as this processing mode is more easily implemented (no phase knowledge is needed). Magnitude mode processing is known to result in a different peak shape[37] (eq 10), and a coefficient $\sqrt{3}$ appears in the relationship between a magnitude mode FWHM and the decay constant (eq 11).

$$L(f) = \frac{1}{\sqrt{4\pi^2(f - f_0)^2 + c^2}} \tag{10}$$

$$\text{FWHM} = \frac{\sqrt{3}\,c}{\pi} \tag{11}$$

However, an additional facet of magnitude mode processing is that it reduces resolution by a factor of 2 as compared to the absorption mode processing,[38] and it is not always possible to obtain complete baseline resolution of closely spaced isotope peaks of highly charged protein ions (Figure S2). The lack of resolving power did not allow accurate determination of FWHM owing to interference between isotope peaks, so measures of peak fitting quality (r^2, chi^2) were not consistent over the entire m/z range of protein ions. Owing to this resolution issue arising from magnitude mode processing, we solely used the absorption mode FT processing for this aspect of the study. However, absorption mode processing requires the frequency spectrum to be properly phased, which is a nontrivial task for FT-MS data. Methods to acquire pure absorption mode spectra have been extensively described in the literature[38−41] and developed into a commercial software package (Autovectis Pro), which was used to generate the spectra for the present study.

For these experiments, the buffer gas pressure in the Orbitrap was maintained at 10^{-10}−10^{-11} mbar. However, as explored in our previous Orbitrap CCS work,[12] the exact value of the pressure and, therefore, the molecule concentration (N), was not known with required precision. To overcome this difficulty, a calibrant ion species was used with a known CCS from IM measurements. As with our previous work, these experiments used the 9+ charge state of ubiquitin as a calibrant, as this ion has been shown to adopt a single conformation in the gas phase.[4]

As already mentioned, the high-energy CCSs measured in FT-ICR and Orbitrap systems are not the same as the cross sections determined by IM and provide, generally speaking, complementary information about the analyte ions. In the scope of this Article, we, however, compare the found CCSs with the IM cross sections through the chosen calibration.

The CCSs determined by the FWHM method showed good agreement with CCSs measured by IM (Figure 1) or values

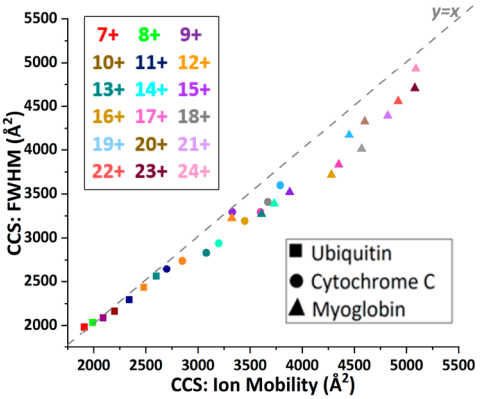

Figure 1. Collision cross sections for myoglobin (charge states 12+ to 24+), cytochrome c (charge states 11+ to 19+), and ubiquitin (charge states 7+ to 13+) determined by the FWHM method versus by ion mobility. A version with error bars and delineation of each charge state for each protein is included as Figure S4.

https://doi.org/10.1021/acs.analchem.2c02146
Anal. Chem. 2022, 94, 15613−15620

determined by our previously reported direct decay profile fitting method (Figure S3, Tables S1−S3) for ion species other than from the calibrant. The CCSs determined by the FWHM method appear close to the decay profile results (Figure S3). They are also in agreement with the IM cross sections with 6% (±4%) precision. The values from the FWHM method slightly underestimate CCS (compared to both IM CCS values and Orbitrap CCSs calculated using the direct decay profile fitting method) in a manner that increases with CCS, which may be attributed to a windowing effect caused by insufficient transient decay in the lower CCS and calibration region, e.g., the lower-CCS data points, including the calibrant ion (ubiquitin 9+), could have overestimated FWHMs resulting in underestimation of the higher CCSs.[16,36] Inherently, the FWHM method will be less accurate than the direct decay profile fitting method, as the FWHM method relies on only three data points (the peak maxima and two points of either side of the peak), whereas the direct decay profile method uses 10−20 data points, as protein ions in this mass range produce 10−20 beats per transient.[12,27] This work lays the foundation for simultaneous measurement of CCS and m/z in applications that employ pure absorption mode spectra in Orbitrap mass analyzers.[42−45] However, these results demonstrate that the FWHM method does not offer a clear advantage in workflows that do not already employ pure absorption mode FT processing in terms of measurement accuracy or computational demand, as only pure absorption mode without apodization can provide accurate FWHMs for CCS measurement, and often, other modes of FT are more commonly used, since they provide higher resolution. We report the results of this method primarily to show that while the FWHM method may seem to be the most logical option for a simple computational method for determination of CCSs from raw files, it is not accurate for RAW files processed using magnitude mode for intact protein ions acquired with isotopic resolution. These results also provide a foundation for the following section aimed at exploring other methods for the determination of CCS from raw files. Therefore, the FWHM method is presented here solely to provide a direct comparison to the direct decay profile fitting method and/or other studies that employ the FWHM method for CCS determination on other FT-MS platforms.

Direct Decay Profile Fitting Method from Raw Files. As the FWHM method produces a wider spread in CCSs for highly charged proteins with closely spaced isotopes as compared to the direct decay profile fitting method and does not offer any computational advantages, we explored other avenues to calculate CCS from spectral files (RAW files). Transients from an Orbitrap mass spectrometer are processed in both absorption and magnitude mode, and instrument software provides users optimized, high-resolution spectra by combining peak shapes of both absorption and magnitude mode peaks, a technique termed Enhanced FT (eFT). As eFT files are not pure absorption mode spectra, this processing does not produce the true Lorentzian peaks needed for the FWHM method.[46] Turning off these commonly used time-to-frequency domain data processing parameters (i.e., Enhanced FT, apodization, and reduced profile mode toggles) allows a pure magnitude mode spectrum to be collected. Here we apply a modified version of the direct decay profile fitting method to calculate CCS from raw files collected in pure magnitude mode. This method was adapted to accommodate magnitude mode data in place of complex FT data when the inverse FT of the peaks of interest is performed.

As previously discussed, the peaks in frequency spectra processed using magnitude mode deviate from true Lorentzian shapes, so some peak distortion is expected when using magnitude mode versus complex FT data. We indeed find this distortion in the resulting decay profiles generated from transients versus RAW files. The decay rate determined from the fit of the decay function from the transient (complex Fourier spectrum) differs from decay rate determined from the exponential decay fit produced from the inverse FT of the RAW file (magnitude mode) on the same experimental data. This deviation is expected as magnitude mode peaks are distorted owing to interference from nearby isotope peaks; however, unlike the FWHM method, the exponential decay fit of the magnitude mode data consistently provided an R^2 of ≥0.99, likely owing measuring time-domain peak maxima instead of measuring the frequency domain FWHM using the FWHM method. The difference between decay rates determined from transients and raw files appears to vary throughout the range of CCS evaluated (spanning 3 proteins and 18 charge states), as evidenced by the deviation between the CCS determined using the raw files/magnitude mode processing and those determined from transients (complex frequency data), as illustrated in Figure S5a. The discrepancy increases with the CCS, resulting in underestimation of CCS by as much as 30%. A similar trend also occurs when comparing the CCSs calculated from the raw files to those determined by ion mobility (Figure 2a), again indicating a systematic underestimation of CCS by as much as 30% based on the raw file method. Both relationships shown in Figures 2a and S5a reveal nonzero y intercepts, and it is possible that the pressure calibration method (based solely on the decay rate of ubiquitin (9+)) in the Orbitrap analyzer is insufficient. Although there is a discrepancy between CCS calculated from raw files and transients, the disagreement follows a predictable near-linear pattern that may be corrected to obtain more accurate CCS values (detailed correction factor information is described in the SI).

The CCSs from the raw file method in Figure 2a were corrected based on application of a linear correction factor with an R^2 of 0.97 to give the corrected CCSs in Figure 2b. With this correction factor, there is significantly better agreement with the CCS values from IM (Figure 2b) as well as with CCSs calculated from transients (Figure S5b, Tables S1−S3). While the raw file method requires a correction factor for accurate CCSs, the method allows greater access to estimation of CCS for any user with an Orbitrap (Elite) mass spectrometer and alleviates the need for access to transients.

Wide-Selected Ion Monitoring (SIM) CCS Measurements. The ease and accuracy of estimating CCS from transients motivated our interest in adapting the strategy for higher-throughput applications, particularly for determining CCS values for multiple charge states or multiple proteins simultaneously. This wide-SIM approach alleviates the need to isolate individual charge states prior to CCS analysis and is advantageous for workflows in which isolation of specific ions is not feasible such as the measurement of ions after supplemental activation is applied to remove adducts or eject monomers. For this wide-SIM method, we opted to use the direct decay profile fitting method over the FWHM method because the direct decay profile fitting method consistently provides more accurate CCSs than the FWHM method (Figure S3). To avoid compounding errors, we did not implement this multiplexing strategy using RAW files. For the

https://doi.org/10.1021/acs.analchem.2c02146
Anal. Chem. 2022, 94, 15613−15620

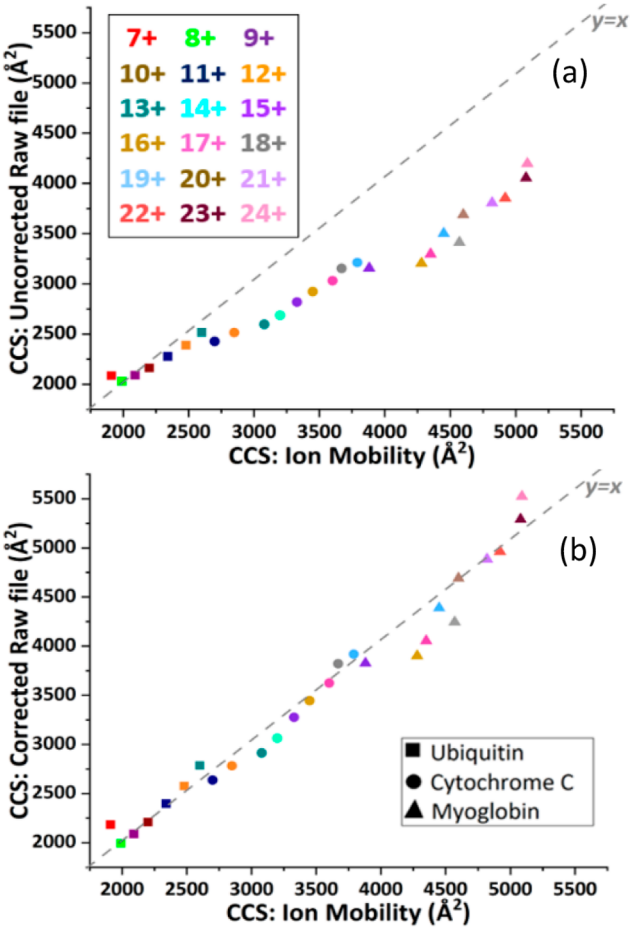

Figure 2. Collision cross sections for myoglobin (charge states 15+ to 24+), cytochrome c (charge states 11+ to 19+), and ubiquitin (charge states 7+ to 13+) determined by the direct decay profile fitting method using raw files (a) without or (b) with a correction factor versus CCS values determined by ion mobility. The dashed line is shown for a $y = x$ correlation. A version with error bars and delineation of each charge state for each protein is included as Figure S6. The correction method used for Figure 2b is described in Supporting Information.

wide-SIM approach, 2−4 charge states of a protein were transferred to the Orbitrap analyzer, and the time-domain transient was recorded and then Fourier transformed to generate a frequency spectrum. We found that experiments with 2−4 charge states were ideal to avoid overfilling the C-trap, which may cause dephasing of ion packets during injection from the C-trap to the Orbitrap, resulting in amplified decay and affording higher than expected CCSs.[47] Simply lowering the AGC target to avoid overfill of C-trap would not provide accurate measurements as the AGC target needs to be around 5E4 for ions to have sufficient signal-to-noise ratio (Figure S1). For data processing of the wide-SIM results, the isotope peaks of a single charge state in the resulting frequency spectrum were shifted to zero frequency and then subjected to inverse Fourier transform to yield a filtered time-domain transient signal which was fit to an exponential decay function. The computational process was repeated to obtain a decay rate for each charge state. As usual, ubiquitin was used as a pressure calibrant to estimate the gas molecule density based on the decay rate of the 9+ charge state. Implementation of the wide-SIM method required calculating the frequencies of ions in each charge state and selecting peaks in that region of the frequency spectrum to ensure that the decay rates corresponded to those charge states.

The CCS values determined via the wide-SIM method are compared to CCS values from ion mobility in Figure 3 for

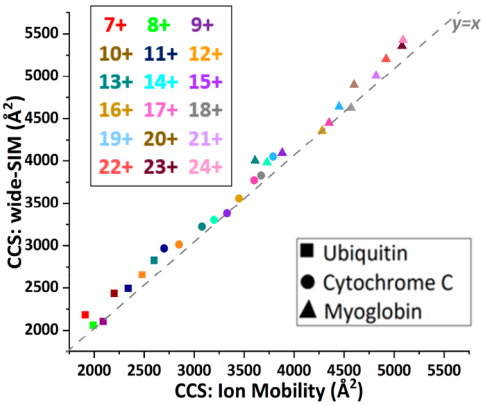

Figure 3. Collision cross section measurements for myoglobin (charge states 14+ to 24+), cytochrome c (charge states 11+ to 19+), and ubiquitin (charge states 7+ to 13+) determined by the wide-SIM direct decay profile fitting method relative to ion mobility for each charge state. Each wide-SIM measurement consisted of 2−4 charge states of the same protein with an isolation width ranging from 50 to 250 m/z. Specific isolation widths for each wide-SIM are included in Table S4. A version with error bars and delineation of each charge state for each protein is included as Figure S8.

ubiquitin, cytochrome c, and myoglobin and similarly compared to those based on evaluation of individual isolated charge states via the direct decay profile fitting method in Figure S7. In general, we found that the CCS values from the wide-SIM strategy showed good agreement (an average of 6 ± 3% error) with IM CCS measurements. The higher deviations in the wide-SIM CCSs may be caused by injecting ions in multiple charge states into the C-trap/Orbitrap at once, which may cause some ions to decay without collisions due to space charge interactions.[27]

We also examined the use of the wide-SIM strategy for measurement of CCS for mixtures containing more than one protein. Mass spectra for a solution containing ubiquitin and cytochrome c used in wide-SIM CCSs measurements are shown in Figure 4a, and the CCS values determined from the wide-SIM method versus ion mobility are plotted in Figure 4b. The error between the CCS values determined by the wide-SIM method relative to CCSs obtained for individual charge states is shown in Figure S9 as well as in Tables S1−S3. The CCS values show good agreement relative to IM CCSs, while again, the slight positive deviation compared to other methods might originate from space charging between ions of different charge states injected into the Orbitrap analyzer at the same time.

For successful wide-SIM measurements, we found that the relative abundances of the ions should be optimized, and each ion's isotope distribution should not overlap with that of other ions. The AGC target was kept at 5E4 as to avoid overfilling of the C-trap. As all ions in a mass spectrum contribute to the AGC target based on their relative abundance and charge, ions that account for less than 10% of the total ion population were found to show artificially increased decay rates owing to faster

https://doi.org/10.1021/acs.analchem.2c02146
Anal. Chem. 2022, 94, 15613−15620

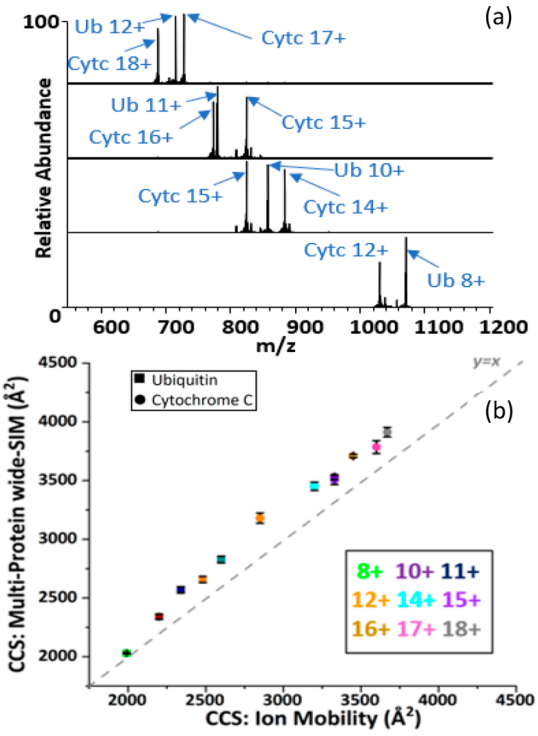

Figure 4. (a) Wide-SIM sections of ESI mass spectra of cytochrome c and ubiquitin in which two or three charge states are isolated at once. (b) Collision cross section measurements for the mixture of ubiquitin (charge states 8+ to 12+) and cytochrome c (charge states 12+ to 18+) determined by the wide-SIM direct decay profile fitting method relative to ion mobility collision cross sections as reference values. The 9+ charge state of ubiquitin and the 13+ charge state of cytochrome c are excluded, as their isotope distributions overlap. Specific isolation widths for each section are included in Table S5.

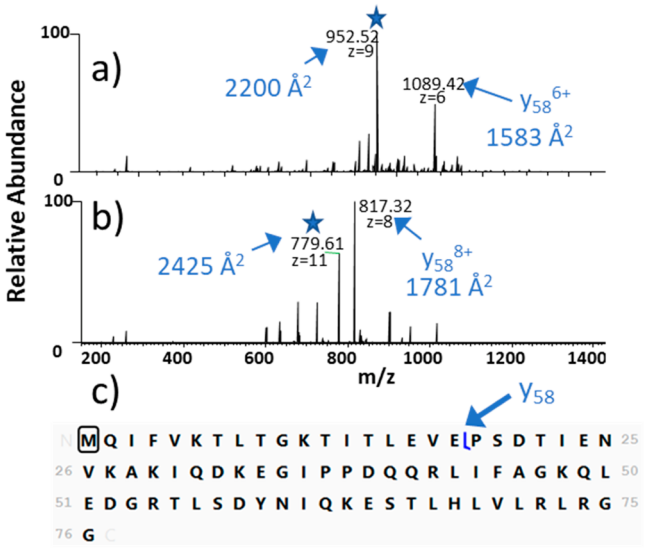

Figure 5. HCD mass spectrum of ubiquitin: (a) 9+ and (b) 11+ charge states. CCSs were generated utilizing a wide-SIM direct decay profile fitting method and are shown for the precursor and selected fragment ions. Each precursor is marked with a star. (c) A sequence map is shown to illustrate the backbone position that is cleaved to generate the y_{58} product ion.

dephasing of their ion packets. However, ions of low relative abundance (<30% of the total ion current) were not investigated in detail in the present study. Another factor to consider when measuring CCS using the wide-SIM method is an ion's position relative to other ions in frequency space. If one ion's isotope distribution overlaps with the isotope distribution of another ion, then their decay rates cannot be distinguished. This confounding issue was encountered in measurements involving the mixture of ubiquitin and cytochrome c, in which the isotope distribution of ubiquitin (9+) and cytochrome c (13+) overlaps, creating merged peaks which are inseparable in frequency space. CCS values for these two ions could not be measured using the wide-SIM mode (and thus are omitted from Figure S9).

Other Applications of Orbitrap CCS Measurements: Fragment Ions and Collision Induced Unfolding. After establishing the wide-SIM method for multiplex measurement of CCS values of ions in different charge states or from different proteins, we investigated the use of wide-SIM measurements for fragments produced by collisional activation of proteins. We applied this strategy for measurement of the CCSs of the high-abundance y_{58} ions generated upon HCD of ubiquitin (9+ and 11+ precursor charge states) (Figure 5). The CCSs of the precursor ions (2200 Å^2 (9+) and 2425 Å^2 (11+)) are in good agreement (5% error) with IM measurements.[5] The CCSs of the y_{58} ions (1583 Å^2 (6+) and 1781 Å^2 (8+)) scale proportionally to their charge state and size relative to the precursor. The difference of ∼200 Å^2 between the two fragment ions is approximately the same as the difference in CCS between the two precursor ions. An analogous experiment was undertaken for selected fragment ions of cytochrome c, revealing similar CCSs for the y_{29}^{3+} ion produced upon CID of two different precursor charge states (11+ and 12+) (Figure S10). For cytochrome c, the CCSs of the precursors (2861 Å^2 (11+) and 2977 Å^2 (12+)) are in good agreement values from ion mobility (2700 Å^2 (11+) and 2850 Å^2 (12+)).[5] Collision activation of both cytochrome c charge states produced the same fragment ion in the same charge state (y_{29}^{3+}), which was found to have similar CCSs when produced from either precursor charge state (1118 and 1202 Å^2 from the 11+ and 12+ charge states of cytochrome c, respectively). These results indicate that wide-SIM methods may be used to measure CCSs of precursor and fragment ions in the same spectrum.

In addition to measuring the CCS of fragment ions produced by CID, we also measured the CCS of intact protein ions after collisional activation. Applying low-energy in-source collisional activation results in collisional heating, a process termed collisional induced unfolding (CIU) that is commonly employed in conjunction with ion mobility measurements to monitor changes in CCS as the protein unfolds.[48] Here we demonstrate that Orbitrap CCS measurements may be used to monitor unfolding of protein ions as demonstrated for cytochrome c (Figure 6). Cytochrome c was analyzed from an aqueous solution (100 mM ammonium acetate) to preserve the native-like compact structure in the gas phase. These experiments were performed on a QE-HFX platform with variable in-source collisional activation applied prior to isolation of the 7+ precursor ion and measurement of CCS in the Orbitrap analyzer using the direct decay profile fitting method. As shown in Figure 6, a low collision voltage (20 V) aids in desolvation but does not unfold the protein as evidenced by little change in the CCS (∼1730 Å^2). Higher collision voltages cause unfolding of the protein, resulting in the observed increases in CCS until a plateau is reached around 1900 Å^2, a rather modest 10% increase in CCS. The

https://doi.org/10.1021/acs.analchem.2c02146
Anal. Chem. 2022, 94, 15613−15620

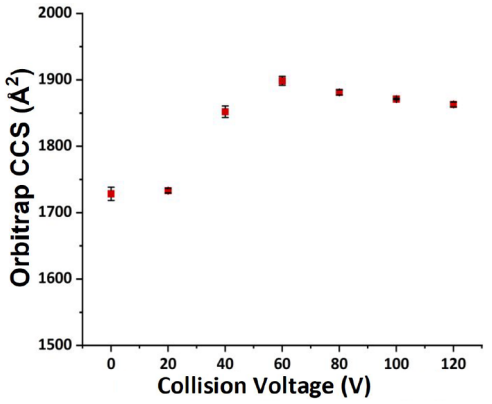

Figure 6. CCS of native-like cytochrome c (7+) relative to the collision energy applied for in-source activation. CCS was calculated using the direct decay profile fitting method for the isolated 7+ charge state.

general CIU profile mirrors one shown in a recent ion mobility/CIU study of cytochrome c (7+ charge state), in which the CCS of the folded protein was 1503 Å^2 prior to exhibiting a transition at higher collision voltages to adopt a series of unfolded structures of around 1950, 2000, and 2100 Å^2, net increases of 30 to 40%.[49] While it appears that the CIU experiments in the Orbitrap mass spectrometer do not result in the same extent of unfolding as IM experiments, the results are not expected to be identical owing to the difference in the experimental details. In particular, for Orbitrap CIU experiments, the ions are collisionally unfolded in the front end of the instrument and have a long path length to the Orbitrap analyzer, during which potentially they may cool or collapse. In conventional IM CIU methods, collisional heating occurs immediately prior to the ions' transit through the drift cell. Even aside from CIU studies, there is a large spread in IM-CCS values reported for native-like folded cytochrome c (7+), ranging from 1503[(49)] to 1790 Å$^{2(S)}$ and others in-between.[4,50] The ability to monitor CIU of native-like proteins offers another avenue for capitalizing on the measurement of CCS values in an Orbitrap analyzer.

CONCLUSION

The methods and guidelines described in this study lay the foundation for measurement of CCS values using Orbitrap analyzers in many laboratories and workflows. The advantages and disadvantages of each method developed or reported in this study are summarized in Table S6, and a side-by-side comparison of CCSs for one charge state of three proteins is given in Table S7 so that future users of these methods may choose which method is most suitable for their data. To reach a larger user-base, we developed a method to calculate CCS from Orbitrap RAW files of an Orbitrap Elite mass spectrometer, thus circumventing the need for access to transient files. To accomplish this goal, we examined the determination of CCS from the FWHM of frequency domain peaks, a strategy that proved successful but required computationally intensive absorption mode FT processing to obtain accurate FWHM measurements for protein ions having closely spaced isotopes. We also modified our previously developed direct decay profile fitting method to accommodate magnitude mode data instead of complex FT data, providing accurate Orbitrap CCS measurements from raw files after inclusion of a correction factor. We also developed a wide-SIM method to determine CCS values of ions in multiple charge states or from different proteins simultaneously as well as for measurement of CCSs of fragment ions from proteins. As shown in Table S7, while the wide-SIM method slightly overestimates CCS values relative to other methods, it can provide key advantages in certain workflows, such as allowing comparisons of CCS values of different proteins in the same solution. Finally, we demonstrated the ability to monitor collision induced unfolding of native-like proteins based on monitoring CCS values as the protein is subjected to collisional heating. Broader access to CCS methods expands the scope of analysis beyond mass alone, providing another dimension of molecular insight for many applications.

ASSOCIATED CONTENT

Supporting Information

The Supporting Information is available free of charge at https://pubs.acs.org/doi/10.1021/acs.analchem.2c02146.

Graphs of CCS values using different methods (FWHM, direct decay profile fitting, correction factor, individual versus wide-SIM), tables of CCS values obtained by IM, and tables of isolation width used for the wide-SIM CCS measurements are provided (PDF)

AUTHOR INFORMATION

Corresponding Author

Jennifer S. Brodbelt − *Department of Chemistry, The University of Texas at Austin, Austin, Texas 78712, United States;* orcid.org/0000-0003-3207-0217; Email: jbrodbelt@cm.utexas.edu

Authors

Virginia K. James − *Department of Chemistry, The University of Texas at Austin, Austin, Texas 78712, United States*

James D. Sanders − *Department of Chemistry, The University of Texas at Austin, Austin, Texas 78712, United States*

Konstantin Aizikov − *Thermo Fisher Scientific, Bremen 28199, Germany*

Kyle L. Fort − *Thermo Fisher Scientific, Bremen 28199, Germany*

Dmitry Grinfeld − *Thermo Fisher Scientific, Bremen 28199, Germany;* orcid.org/0000-0003-2261-4209

Alexander Makarov − *Thermo Fisher Scientific, Bremen 28199, Germany; Biomolecular Mass Spectrometry and Proteomics, Bijvoet Center for Biomolecular Research and Utrecht Institute for Pharmaceutical Sciences, University of Utrecht, Utrecht 3584, The Netherlands;* orcid.org/0000-0002-7046-6709

Complete contact information is available at: https://pubs.acs.org/10.1021/acs.analchem.2c02146

Notes

The authors declare the following competing financial interest(s): four authors (Aizikov, Fort, Grinfeld, Makarov) are employees of Thermo Fisher Scientific, the developers of the Orbitrap mass spectrometer used for the study.

ACKNOWLEDGMENTS

We acknowledge the following funding sources: NSF (Grant CHE-2203602) and the Welch Foundation (Grant F-1155). Drs. Yuri Tsybin, Konstantin Nagornov and David Kilgour are

acknowledged for their guidance on the use of Autovectis Pro to obtain the absorption mode spectra.

REFERENCES

(1) Wyttenbach, T.; von Helden, G.; Bowers, M. T. *J. Am. Chem. Soc.* **1996**, *118* (35), 8355−8364.
(2) Ewing, M. A.; Glover, M. S.; Clemmer, D. E. *J. Chromatogr. A* **2016**, *1439*, 3−25.
(3) Hinnenkamp, V.; Klein, J.; Meckelmann, S. W.; Balsaa, P.; Schmidt, T. C.; Schmitz, O. J. *Anal. Chem.* **2018**, *90* (20), 12042−12050.
(4) May, J. C.; Jurneczko, E.; Stow, S. M.; Kratochvil, I.; Kalkhof, S.; McLean, J. A. *Int. J. Mass Spectrom.* **2018**, *427*, 79−90.
(5) Bush, M. F.; Hall, Z.; Giles, K.; Hoyes, J.; Robinson, C. V.; Ruotolo, B. T. *Anal. Chem.* **2010**, *82* (22), 9557−9565.
(6) Pukala, T. *Rapid Commun. Mass Spectrom.* **2019**, *33* (S3), 72−82.
(7) Goh, C.-S.; Milburn, D.; Gerstein, M. *Curr. Opin. Struct. Biol.* **2004**, *14* (1), 104−109.
(8) Soto, C. *FEBS Lett.* **2001**, *498* (2), 204−207.
(9) Gui, M.; Song, W.; Zhou, H.; Xu, J.; Chen, S.; Xiang, Y.; Wang, X. *Cell Res.* **2017**, *27* (1), 119−129.
(10) Dodds, J. N.; Baker, E. S. *J. Am. Soc. Mass Spectrom.* **2019**, *30* (11), 2185−2195.
(11) Gabelica, V.; Marklund, E. *Curr. Opin. Chem. Biol.* **2018**, *42*, 51−59.
(12) Sanders, J. D.; Grinfeld, D.; Aizikov, K.; Makarov, A.; Holden, D. D.; Brodbelt, J. S. *Anal. Chem.* **2018**, *90* (9), 5896−5902.
(13) Jones, C. A.; Dearden, D. V. *J. Am. Soc. Mass Spectrom.* **2015**, *26* (2), 323−329.
(14) Yang, F.; Voelkel, J. E.; Dearden, D. V. *Anal. Chem.* **2012**, *84* (11), 4851−4857.
(15) Anupriya; Gustafson, E.; Mortensen, D. N.; Dearden, D. V. *J. Am. Soc. Mass Spectrom.* **2018**, *29* (2), 251−259.
(16) Jiang, T.; Chen, Y.; Mao, L.; Marshall, A. G.; Xu, W. *Phys. Chem. Chem. Phys.* **2016**, *18* (2), 713−717.
(17) Guo, D.; Xin, Y.; Li, D.; Xu, W. *Phys. Chem. Chem. Phys. PCCP* **2015**, *17* (14), 9060−9067.
(18) Wobschall, D.; Graham, J. R.; Malone, D. P. *Phys. Rev.* **1963**, *131* (4), 1565−1571.
(19) Wobschall, D.; Fluegge, R. A.; Graham, J. R. *J. Chem. Phys.* **1967**, *47* (10), 4091−4094.
(20) Huntress, W. T. *J. Chem. Phys.* **1971**, *55* (5), 2146−2155.
(21) Dymerski, P. P.; Dunbar, R. C. *J. Chem. Phys.* **1972**, *57* (9), 4049−4050.
(22) Dziekonski, E. T.; Johnson, J. T.; Lee, K. W.; McLuckey, S. A. *J. Am. Soc. Mass Spectrom.* **2018**, *29* (2), 242−250.
(23) Elliott, A. G.; Harper, C. C.; Lin, H.-W.; Susa, A. C.; Xia, Z.; Williams, E. R. *Anal. Chem.* **2017**, *89* (14), 7701−7708.
(24) Hu, M.; Zhang, L.; He, S.; Xu, C.; Shi, Q. *Rapid Commun. Mass Spectrom.* **2018**, *32* (9), 751−761.
(25) Shrestha, J.; Porter, S. R.; Tinsley, C.; Arslanian, A. J.; Dearden, D. V. *J. Phys. Chem. A* **2022**, *126* (19), 2950−2958.
(26) Arslanian, A. J.; Mismash, N.; Dearden, D. V. *J. Am. Soc. Mass Spectrom.* **2022**, *33* (9), 1626−1635.
(27) Makarov, A.; Denisov, E. *J. Am. Soc. Mass Spectrom.* **2009**, *20* (8), 1486−1495.
(28) Zhou, M.; Jiao, L.; Xu, S.; Xu, Y.; Du, M.; Zhang, X.; Kong, X. *Rev. Sci. Instrum.* **2022**, *93* (4), 043003.
(29) Naylor, C. N.; Reinecke, T.; Clowers, B. H. *Anal. Chem.* **2020**, *92* (6), 4226−4234.
(30) Hill, H. H.; Hill, C. H.; Asbury, G. R.; Wu, C.; Matz, L. M.; Ichiye, T. *Int. J. Mass Spectrom.* **2002**, *219* (1), 23−37.
(31) Asbury, G. R.; Hill, H. H. *Anal. Chem.* **2000**, *72* (3), 580−584.
(32) Heravi, T.; Arslanian, A. J.; Johnson, S. D.; Dearden, D. V. *J. Am. Soc. Mass Spectrom.* **2022**, *33* (9), 1644−1652.
(33) Guzmán, U. H.; Fort, K.; Aizikov, K.; Rykaer, M.; Madsen, J.; Martínez-Val, A.; Makarov, A.; Olsen, J. Inference of Collisional Cross-Sections of Peptides in an Orbitrap Mass Analyzer. *Proceedings of the 69th ASMS Conference on Mass Spectrometry and Allied Topics*, 2021.
(34) Pope, B. L.; Joaquin, D.; Hickey, J. T.; Mismash, N.; Heravi, T.; Shrestha, J.; Arslanian, A. J.; Anupriya; Mortensen, D. N.; Dearden, D. V. *J. Am. Soc. Mass Spectrom.* **2022**, *33* (1), 131−140.
(35) Pope, B. L.; Joaquin, D.; Hickey, J. T.; Mismash, N.; Heravi, T.; Shrestha, J.; Arslanian, A. J.; Anupriya; Mortensen, D. N.; Dearden, D. V. *J. Am. Soc. Mass Spectrom.* **2022**, *33*, 131.
(36) Li, D.; Tang, Y.; Xu, W. *Analyst* **2016**, *141* (12), 3554−3561.
(37) Chen, L.; Cottrell, C. E.; Marshall, A. G. *Chemom. Intell. Lab. Syst.* **1986**, *1* (1), 51−58.
(38) Kilgour, D. P. A.; Wills, R.; Qi, Y.; O'Connor, P. B. *Anal. Chem.* **2013**, *85* (8), 3903−3911.
(39) Qi, Y.; Barrow, M. P.; Li, H.; Meier, J. E.; Van Orden, S. L.; Thompson, C. J.; O'Connor, P. B. *Anal. Chem.* **2012**, *84* (6), 2923−2929.
(40) Kilgour, D. P. A.; Nagornov, K. O.; Kozhinov, A. N.; Zhurov, K. O.; Tsybin, Y. O. *Rapid Commun. Mass Spectrom.* **2015**, *29* (11), 1087−1093.
(41) Qi, Y.; Li, H.; Wills, R. H.; Perez-Hurtado, P.; Yu, X.; Kilgour, D. P. A.; Barrow, M. P.; Lin, C.; O'Connor, P. B. *J. Am. Soc. Mass Spectrom.* **2013**, *24* (6), 828−834.
(42) Nagornov, K. O.; Zennegg, M.; Kozhinov, A. N.; Tsybin, Y. O.; Bleiner, D. *J. Am. Soc. Mass Spectrom.* **2020**, *31* (2), 257−266.
(43) Nagornov, K. O.; Gasilova, N.; Kozhinov, A. N.; Virta, P.; Holm, P.; Menin, L.; Nesatyy, V. J.; Tsybin, Y. O. *Anal. Chem.* **2021**, *93* (38), 12930−12937.
(44) Kösling, P.; Rüger, C. P.; Schade, J.; Fort, K. L.; Ehlert, S.; Irsig, R.; Kozhinov, A. N.; Nagornov, K. O.; Makarov, A.; Rigler, M.; Tsybin, Y. O.; Walte, A.; Zimmermann, R. *Anal. Chem.* **2021**, *93* (27), 9418−9427.
(45) Bills, J. R.; Nagornov, K. O.; Kozhinov, A. N.; Williams, T. J.; Tsybin, Y. O.; Marcus, R. K. *J. Am. Soc. Mass Spectrom.* **2021**, *32* (5), 1224−1236.
(46) Lange, O.; Damoc, E.; Wieghaus, A.; Makarov, A. *Int. J. Mass Spectrom.* **2014**, *369*, 16−22.
(47) Grinfeld, D. E.; Kopaev, I. A.; Makarov, A. A.; Monastyrskiy, M. A. *Nucl. Instrum. Methods Phys. Res. Sect. Accel. Spectrometers Detect. Assoc. Equip.* **2011**, *645* (1), 141−145.
(48) Dixit, S. M.; Polasky, D. A.; Ruotolo, B. T. *Curr. Opin. Chem. Biol.* **2018**, *42*, 93−100.
(49) Borotto, N. B.; Osho, K. E.; Richards, T. K.; Graham, K. A. *J. Am. Soc. Mass Spectrom.* **2022**, *33* (1), 83−89.
(50) Laszlo, K. J.; Buckner, J. H.; Munger, E. B.; Bush, M. F. *J. Am. Soc. Mass Spectrom.* **2017**, *28* (7), 1382−1391.

https://doi.org/10.1021/acs.analchem.2c02146
Anal. Chem. 2022, 94, 15613−15620